Electric-Field Modulation of Amyloid-Beta–Membrane Interactions by AC0107 and Bexarotene: An Atomistic Molecular Dynamics Study

Nafiseh Salehi[a], Amir Lohrasebi[b,*]

[a] Department of Chemistry, University of Isfahan, Isfahan 81746-73441, Iran

[b] Department of Physics, University of Isfahan, Isfahan 81746-73441, Iran

Abstract

Alzheimer's disease is closely associated with the interaction and aggregation of amyloid-beta (Aβ) peptides at neuronal membranes. Here, we use atomistic molecular dynamics simulations to investigate how two Aβ-interacting molecules, AC0107 and bexarotene, modulate Aβ–membrane interactions in a cholesterol-enriched POPC bilayer, with and without an oscillating GHz electric field. Five simulation conditions were examined, and peptide structural stability, membrane ordering, mobility, hydrogen bonding, radial distribution, and mass-density profiles were analyzed. The results reveal distinct modes of action for the two molecules. AC0107 preferentially localizes near the membrane–peptide interface and increases peptide–membrane hydrogen bonding, consistent with a barrier-like mechanism at the membrane surface. In contrast, bexarotene preferentially associates with the peptide when combined with the electric field, reduces peptide–membrane hydrogen bonding, and produces a more pronounced decrease in peptide mobility. The electric field therefore modulates the effects of the two compounds in different ways, enhancing the membrane-protective behavior of bexarotene while altering the response of AC0107. Overall, the simulations provide molecular-level insight into how small-molecule localization and external electric fields can regulate Aβ–membrane interactions.

Keywords: Atomistic molecular dynamics, Cholesterol-enriched POPC bilayer, Oscillating GHz electric field, Peptide–membrane, Alzheimer's disease

*__Corresponding Authors:__

Amir Lohrasebi, E-mail: lohrasebi@phys.ui.ac.ir

The corresponding author's ORCID: 0000-0002-7022-2237

Abbreviations

AD	Alzheimer Disease
Aβ	Amyloid-beta
POPC	palmitoyl-oleoyl-phosphatidylcholine
MD	Molecular Dynamics
MSD	Mean-Square Displacement
RDF	Radial Distribution Function
[AC0107]	Drug molecule (4-({[3-(1-Pyrrolidinylmethyl) benzyl] amino} methyl) benzon)
Bexarotene	Drug molecule (4-[1-(3,5,5,8,8-pentamethyl-6,7-dihydronaphthalen-2-yl) ethenyl] benzoic acid)
RMSD	Root-mean-square deviation
RMSF	Root-mean-square fluctuations
Rg	Radius of gyration
S_{CD}	Order parameter
DFT	Density Functional Theory
PME	particle-mesh Ewald
ATB	Automated Topology Builder
PDB	Protein Data Bank
NPT	Isothermal–Tsobaric Ensemble
SPC/E	extended simple point charge water model
ApoE	apolipoprotein E

1 Introduction

Alzheimer's disease (AD) is a progressive neurodegenerative disorder in which the accumulation and aggregation of Aβ-peptides are closely associated with pathological changes in neuronal tissues. The amyloid cascade hypothesis has therefore motivated extensive efforts to understand the molecular mechanisms underlying Aβ aggregation and to identify strategies for interfering with the formation and membrane association of toxic Aβ assemblies [1–3]. Although Aβ aggregation can occur in aqueous environments, interactions with neuronal membranes provide an important additional factor that can influence peptide conformation, localization, and aggregation behavior. The lipid composition of the membrane, particularly the presence of cholesterol, can substantially modify the association of Aβ with the membrane and consequently influence the formation of membrane-associated assemblies [4]. These observations have stimulated considerable interest in small molecules capable of modulating Aβ aggregation and its interaction with lipid membranes. MD simulations provide an effective

atomistic framework for investigating such processes and for identifying intermolecular interactions that may be difficult to resolve experimentally. A variety of small molecules have been investigated computationally for their ability to modify Aβ structure, oligomerization, and membrane association [5,6]. Among these compounds, AC0107 was identified as a computationally designed molecule capable of interfering with toxic Aβ oligomer formation, with its activity subsequently supported by experimental and molecular-modeling studies [4, 7]. Bexarotene, originally developed as an anticancer compound, has also attracted attention in the context of Aβ-related processes [8]. In an AD mouse model, bexarotene treatment was reported to enhance the ApoE-dependent clearance of soluble Aβ, suggesting an indirect mechanism involving the regulation of Aβ clearance pathways [9]. In a separate study, Fantini et al. demonstrated that bexarotene can interact directly with Aβ peptides and inhibit cholesterol-dependent calcium flux associated with Aβ-derived membrane pores [10]. These findings suggest that bexarotene may influence Aβ-related processes through distinct mechanisms, including the modulation of Aβ clearance and direct effects on Aβ–membrane interactions. Together with AC0107, bexarotene therefore provides an interesting compound for investigating how different small molecules modulate membrane-associated Aβ assemblies.

Our previous molecular modeling study demonstrated that membrane cholesterol and AC0107 can significantly affect the aggregation behavior of Aβ assemblies at lipid membranes. In particular, cholesterol altered the membrane environment experienced by the peptide, while AC0107 modified the tendency of Aβ assemblies to interact with the membrane [4]. More recently, we showed that an oscillating electric field with an amplitude of 70 mV/nm and a frequency of 1 GHz can modify Aβ accumulation at the membrane and alter peptide–lipid interactions [11]. These findings suggest that both chemical modulation by small molecules and physical perturbation by external electric fields can influence the behavior of membrane-associated Aβ. External electric fields can affect biomolecular systems by modifying molecular orientation, electrostatic interactions, membrane organization, and protein–lipid coupling [12-14]. Previous studies have specifically demonstrated that electric or electromagnetic fields can alter the conformational dynamics and aggregation propensity of amyloid peptides [15,16]. Our earlier simulations of membrane-associated Aβ further indicated that a GHz electric field can reduce peptide accumulation at the membrane under the investigated conditions [11]. However, the response of a membrane-associated Aβ system to an electric field may depend strongly on the molecular environment created by an interacting small molecule.

An important question that therefore remains insufficiently explored is whether an external electric field can differentially modify the molecular mechanisms through which distinct Aβ-interacting compounds regulate peptide–membrane interactions. In particular, compounds with different physicochemical properties may occupy different regions of the peptide–membrane interface and consequently respond differently to the same external perturbation. A molecular-level comparison of such effects can provide insight into the coupling between drug localization, membrane organization, peptide mobility, and external-field response.

In the present study, we investigate the effects of AC0107 and bexarotene on membrane-associated Aβ oligomers using atomistic molecular dynamics simulations in a cholesterol-enriched POPC bilayer. The influence of an oscillating electric field with an amplitude of 70 mV/nm and a frequency of 1 GHz is examined for each compound. Five computational conditions are considered to distinguish the effects of the two compounds and their responses to the applied field. Peptide structural stability, membrane ordering, apparent peptide mobility, mass-density profiles, hydrogen bonding, and radial distribution functions are analyzed to establish relationships between molecular localization and Aβ–membrane interactions. Particular attention is given to the different spatial distributions of AC0107 and bexarotene and to how the electric field modifies their interaction patterns. Through this comparative analysis, we aim to provide a molecular-level description of the distinct mechanisms by which these two compounds modulate membrane-associated Aβ under an external electric-field perturbation.

2 Computational Details

2.1. System construction

A cholesterol-enriched phospholipid bilayer was constructed to provide a membrane environment for the Aβ oligomer. The bilayer consisted of 127 POPC molecules and 50 cholesterol molecules, corresponding to approximately 20 wt% cholesterol. Water molecules were added to both sides of the bilayer, resulting in a total of 12,500 water molecules. Five sodium ions were included to maintain charge neutrality. The Aβ oligomer structure used in all simulations was obtained from the Protein Data Bank (PDB ID: 2BEG). The peptide was initially positioned at one side of the cholesterol-enriched membrane. The resulting systems were subsequently prepared for molecular dynamics simulations under the conditions described below.

2.2. Drug structure preparation

The initial molecular structures of AC0107 and bexarotene were obtained from the ZINC20 database using the identifiers ZINC48709826 and ZINC1539579, respectively. The molecular structures were subsequently processed using Gaussian for DFT calculations with the selected functional and basis set used in the original calculations. These calculations were employed to obtain the relevant electronic-structure information and partial atomic charges. The molecular topologies and force-field parameters were generated using the ATB server [17]. The resulting topology files were incorporated into the GROMACS simulation systems, and the molecular dynamics simulations were performed using GROMACS version 5.1.5 with the GROMOS 54A7 force field. The two compounds investigated in this study were AC0107 and bexarotene. Their molecular structures are shown in Fig. 1-a and 1-b panels [7,18]. The system configuration classifications are summarized in Table 1.

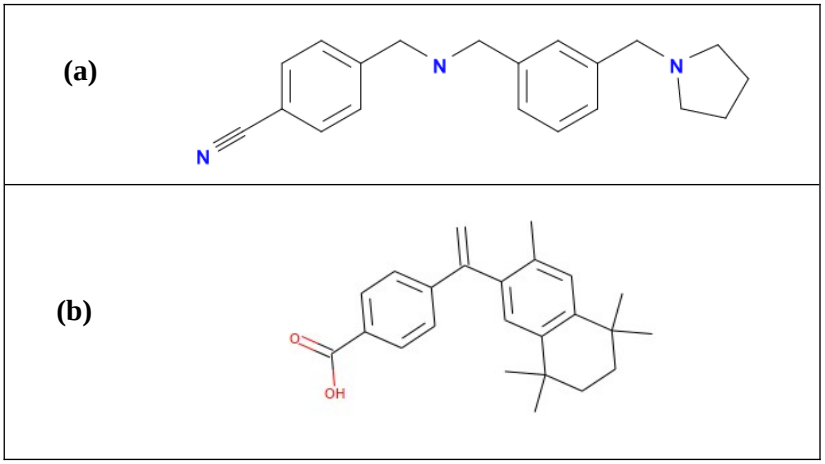


Figure (1) (a) The **s**tructure of the [AC0107] molecule (4-({[3-(1-pyrrolidinylmethyl) benzyl] amino} methyl) benzonitrile). (b) The structure of the Bexarotene molecule (4-[1-(3,5,5,8,8-pentamethyl-6,7-dihydronaphthalen-2-yl) ethenyl] benzoic acid).

Table 1. Five computational setups were considered in different simulations.

system	Electric field	[AC0107] (drug1)	Bexarotene (drug2)
Case-I			
Case-II		√	
Case-III			√
Case-IV	√	√	
Case-V	√		√

2.3. Molecular dynamics simulations

All molecular dynamics simulations were performed using GROMACS version 5.1.5 with and the parameters of GROMOS 54A7 force field [19] and SPC/E [20] water model was used to calculate the interactions between the atoms in the system. The PME method [21] was employed to compute the electrostatic interactions and the cutoff radius of van der Waals and Columbic interactions has been set to 1.2 nm and the simulation time step was set at 1 fs.The systems were simulated in the NPT ensemble and the Nose–Hoover thermostat [22] andParrinello–Rahman barostat [23] were used to maintain the temperature and pressure at $310K$ and 1 atm, representing near-physiological temperature and pressure conditions. Temperature regulation was performed using the velocity-rescaling (v-rescale) thermostat, while pressure was controlled using the Berendsen barostat. For each computational condition, the system was first equilibrated for 200 ns. This was followed by an additional 200 ns production simulation, giving a total simulation time of 400 ns for each condition. The production trajectories were subsequently used for the structural, dynamical, and intermolecular analyses described in Section 3. Five computational conditions were considered in order to distinguish the effects of the two compounds and the applied electric field. Case I represents the membrane-associated Aβ system without the oscillating electric field and either compound. Cases II and III correspond to the systems containing AC0107 and bexarotene, respectively, without the electric field. Cases IV and V contain AC0107 and bexarotene, respectively, in combination with the electric field. The complete arrangement of the five systems is given in Table 1 and illustrated schematically in Figure 2. An oscillating external electric field with an amplitude of 70 mV/nm and a frequency of 1 GHz was applied to the selected simulation systems [11]. The field was applied in Cases IV, and V, whereas Cases I, II and III were simulated in the absence of the external field. In the present study, the electric field is considered as a controlled molecular-scale perturbation introduced to examine how an oscillatory electromagnetic environment modifies the interaction network among the Aβ oligomer, the lipid membrane, and the small molecules.

2.3. Structural and intermolecular analyses

The structural stability and conformational behavior of the Aβ oligomer were characterized using the RMSD, RMSF, and Rg. RMSD was used to monitor the temporal evolution of the overall peptide structure, whereas RMSF was used to characterize local fluctuations. The radius of gyration was evaluated as a measure of the global compactness of the peptide assembly. The response of the lipid bilayer was characterized using the deuterium order parameter, SCD, for the palmitoyl and oleoyl chains of POPC. The translational behavior of the Aβ oligomer was examined using the MSD.

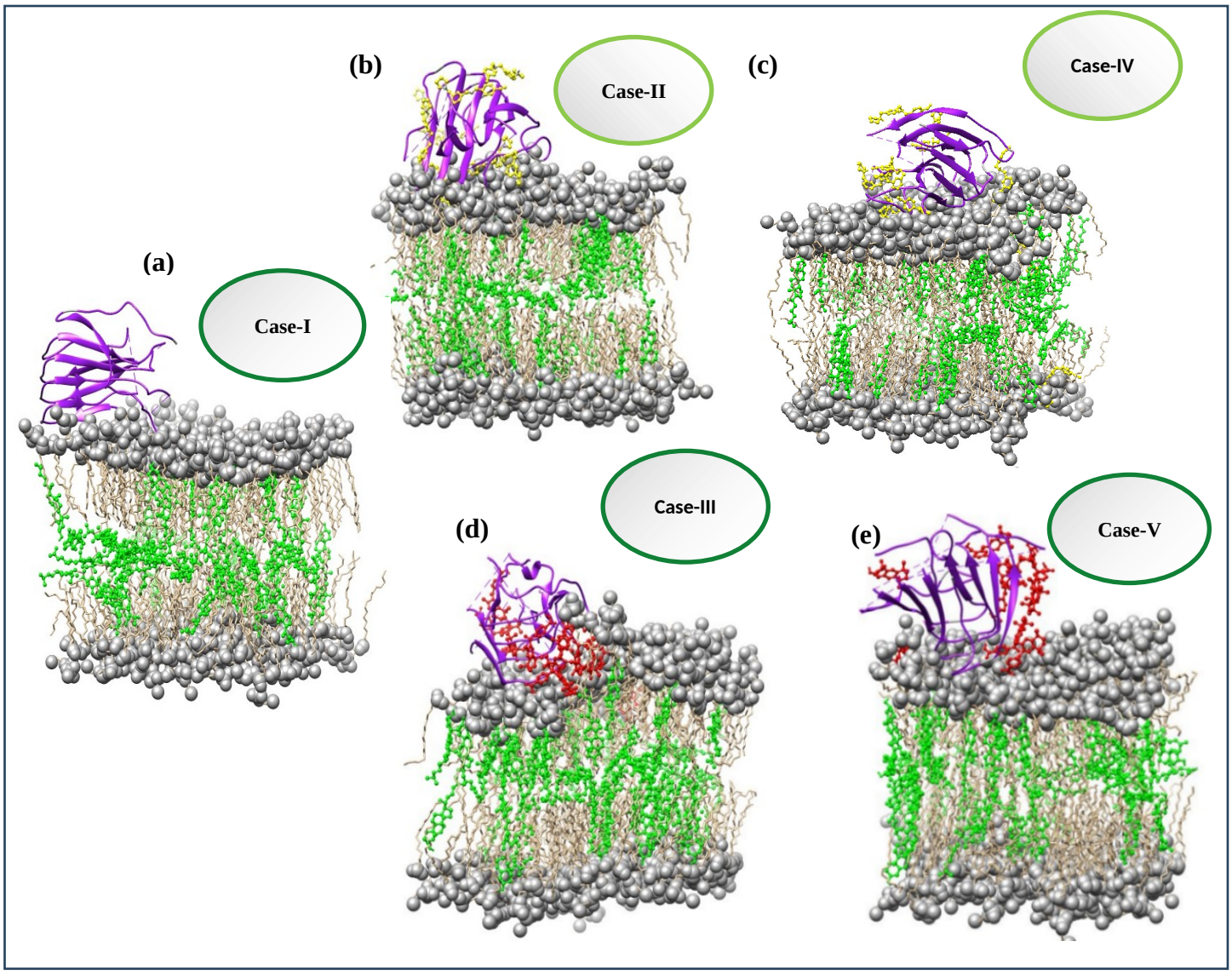


Figure (2) Five different cases' arrangement of the system contained the Aβ oligomers on top of the cholesterol-enriched membrane. (a) Case-I, the system without the electric field and drugs. (b) Case-II, the system with the first drug [AC0107]. (c) Case-III, the system with the second drug, bexarotene. (d) Case-IV, the system with the first drug, under the application of the electric field. (e) Case-V, the system with the second drug and the electric field.

This analysis was used to evaluate changes in lipid-chain ordering resulting from the presence of the compounds and/or the applied electric field. It is well known that RMSD is described as a measure of structural deviation from a reference conformation over time; RMSF characterizes local atomic or residue-level fluctuations; and the radius of gyration reflects the overall compactness of the peptide assembly. Mass-density profiles are used to examine the spatial distribution of selected components along the membrane-normal direction, whereas RDFs characterize the relative spatial probability of selected atom groups as a function of separation. The final 20 ns of each production trajectory were used for the comparative mobility analysis, and the corresponding linear-region values are reported in Table 2. Because each condition was represented by a single trajectory, these quantities are interpreted primarily as trajectory-based comparative mobility measures rather than fully converged ensemble transport coefficients. Spatial distributions within the systems were characterized using mass-density profiles and RDFs. The mass-density analysis was used to examine the relative localization of the Aβ oligomer, the compounds, and membrane components along the membrane-normal direction. RDF analysis was further used to characterize the spatial relationships among selected peptide, drug, and membrane atoms. Hydrogen bonds between Aβ and POPC, between the drug molecules and POPC, and between the drug molecules and Aβ were also analyzed. The reported values correspond to the final 20 ns of each production trajectory. These analyses were combined with the structural and spatial descriptors to provide a molecular-level interpretation of the interactions governing the behavior of the membrane-associated Aβ oligomer.

2.4. Sampling and interpretation of the trajectories

Each computational condition was represented by one molecular dynamics trajectory consisting of 200 ns equilibration followed by 200 ns production. The relatively long trajectory for each system was selected to allow the systems to evolve over an extended timescale and to examine the persistence of the observed structural and intermolecular trends. Because independent replicas were not generated for the individual conditions, the results are interpreted primarily through cross-analysis of complementary observables rather than formal statistical comparison between independent trajectories. The consistency among structural stability, membrane ordering, mobility, spatial distribution, hydrogen bonding, and RDF analyses provides the basis for the mechanistic interpretation presented in the Results and Discussion section.

3 Results and Discussion

3.1. Structural stability and conformational response of Aβ

To examine the structural response of the Aβ oligomer under the five simulated conditions, RMSD, RMSF, and Rg were analyzed. These descriptors provide complementary information on the temporal stability, local flexibility, and global compactness of the peptide assembly.

The RMSD profiles presented in Fig. 3 show that the Aβ oligomer remains relatively stable throughout the production simulations in all five conditions.

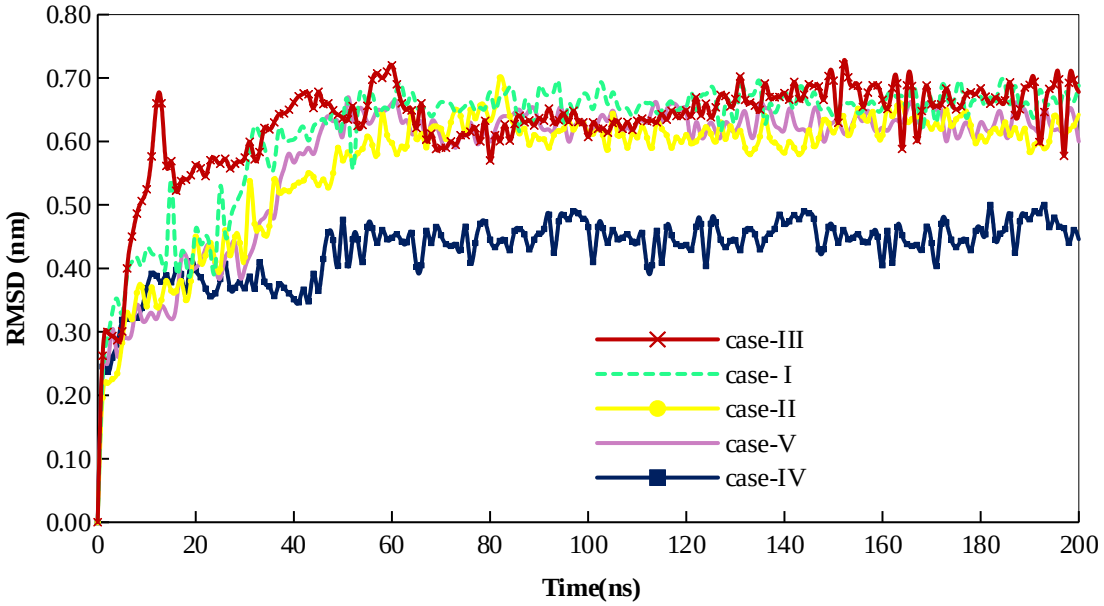


Figure (3) Root mean square deviation of Aβ peptide plotted as a function of time for the five different cases.

No pronounced long-term structural drift is observed, indicating that the peptide maintains its overall structural framework during the simulated period. The similarities among the RMSD profiles also suggest that the main differences between the investigated conditions are associated with changes in peptide–membrane and peptide–drug interactions rather than with a complete restructuring of the oligomer.

The local flexibility of the peptide was further examined using RMSF analysis (Figure 4). Lower fluctuations are observed in Cases I, III, and V, whereas the presence of AC0107 in Case II is associated with increased fluctuations in several flexible regions of the peptide. This behavior suggests that AC0107 modifies the local conformational dynamics of Aβ while leaving its overall structural organization largely preserved. By comparison, the RMSF profiles of the systems containing bexarotene indicate comparatively restricted local fluctuations. The

relatively small differences between systems with and without the electric field also suggest that the field does not produce a major additional change in residue-level flexibility under the conditions investigated.

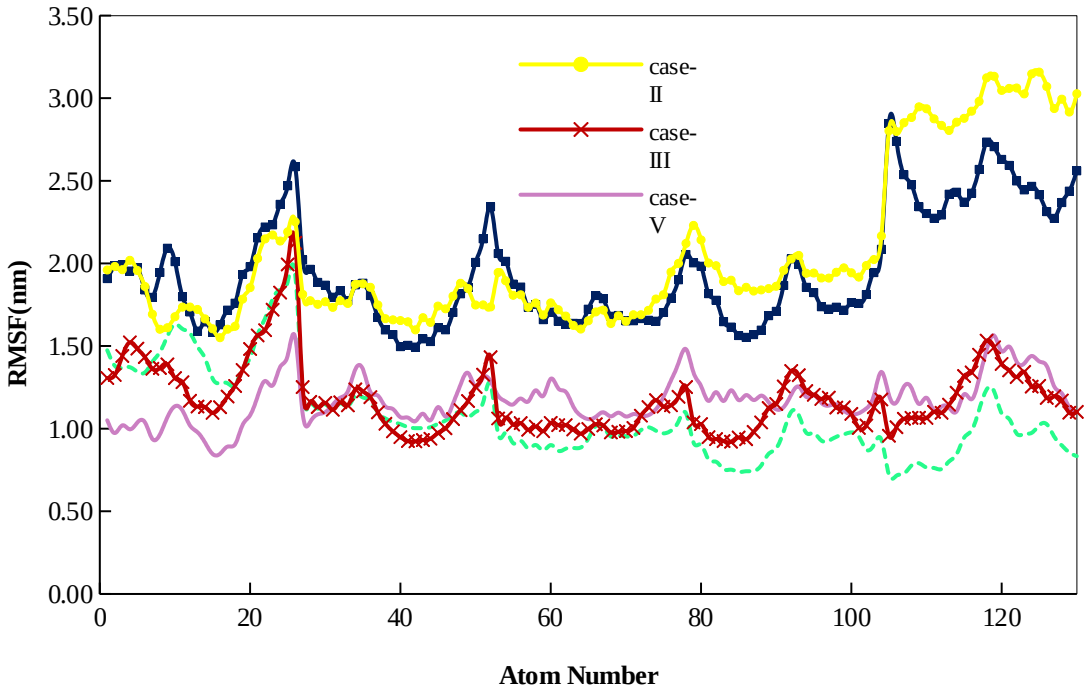


Figure (4) RMSF values for the carbon skeleton atoms of the Aβ oligomer peptide, for the five different cases.

The radius of gyration provides an additional measure of the global dimensions of the oligomer. The final Rg values are 1.39, 1.41, 1.36, 1.39, and 1.39 nm for Cases I–V, respectively. The nearly identical values for Cases IV and V indicate that the electric field does not substantially alter the overall compactness of the Aβ oligomer. The slightly higher Rg in Case II and lower value in Case III suggest that AC0107 and bexarotene affect the global organization of the peptide differently, although the magnitude of these changes remains relatively small.

Taken together, the RMSD, RMSF, and Rg analyses indicate that the two compounds modulate Aβ dynamics without causing a major disruption of its overall structural framework. An important distinction nevertheless emerges: AC0107 is associated with enhanced local conformational flexibility, whereas bexarotene produces comparatively restricted peptide fluctuations. These structural observations provide a basis for examining how the two compounds influence membrane organization and peptide mobility.

3.2. Effect of the compounds and electric field on membrane organization

Because membrane organization can influence the interaction of Aβ with the lipid bilayer, the order parameter S_{CD} of the POPC hydrocarbon chains was calculated for the palmitoyl and oleoyl branches. The results are shown in Figure 5.

The order-parameter profiles indicate that both molecular composition and electric-field exposure affect lipid-chain organization. The presence of AC0107 in Case II produces a noticeable increase in membrane ordering compared with the corresponding systems. When the electric field is applied in the presence of AC0107 (Case IV), this ordering is reduced relative to Case II. The bexarotene-containing systems also exhibit field-dependent changes in membrane order, although their response differs from that observed for AC0107. These findings indicate that the applied electric field does not simply produce a uniform increase or decrease in membrane ordering. Instead, its effect depends on the molecular environment established by the interacting compound. The different responses of the membrane to AC0107 and bexarotene are therefore consistent with the possibility that the two compounds occupy different regions of the peptide–membrane interface and establish different interaction networks.

This observation is particularly relevant to the central objective of the present study, because changes in lipid ordering can alter the physical environment experienced by a membrane-associated Aβ oligomer. The membrane response therefore provides an intermediate link between the applied electric field and the subsequent changes observed in peptide mobility and peptide–membrane interactions.

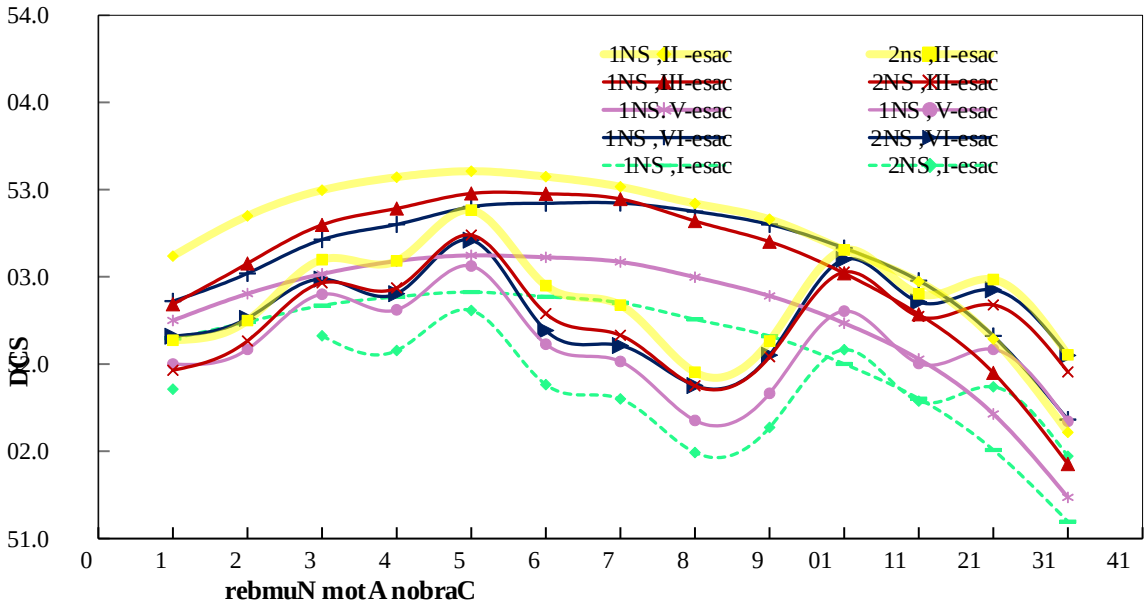


Figure (5) Average order parameter of palmitoyl and oleoyl chains of POPC lipid molecules for the five different cases.

3.3. Aβ mobility from mean-square displacement analysis

To characterize the translational behavior of the membrane-associated Aβ oligomer, the MSD was calculated. The MSD curves obtained over the final 20 ns of the production trajectories are presented in Fig. 6, and the corresponding values are summarized in Table 2.

For the system of Case I, the MSD-derived apparent mobility coefficient is 2.197×10^{-5} cm²/s. In the presence of AC0107 without the electric field (Case II), this value decreases to 1.832×10^{-5} cm²/s. Thus, although AC0107 increases local peptide fluctuations according to the RMSF analysis, it is associated with a modest reduction in the overall translational mobility of the oligomer. These two observations are not contradictory: increased local flexibility describes internal conformational motion, whereas the MSD reflects the displacement of the peptide assembly as a whole. In contrast, bexarotene in the absence of the electric field (Case III) yields the largest apparent mobility coefficient, 2.957×10^{-5} cm²/s. This enhanced mobility is consistent with the reduced direct interaction of the peptide with the membrane observed in the hydrogen-bond and spatial-distribution analyses discussed below.

A pronounced reduction in the MSD-derived mobility is observed when the electric field is applied. The value decreases to 0.132×10^{-5} cm²/s in the AC0107-containing system (Case IV) and to 0.027×10^{-5} cm²/s in the bexarotene-containing system (Case V). The particularly strong reduction in Case V indicates that the combined presence of bexarotene and the electric field produces a substantially more restricted translational response of the peptide than the other investigated conditions.

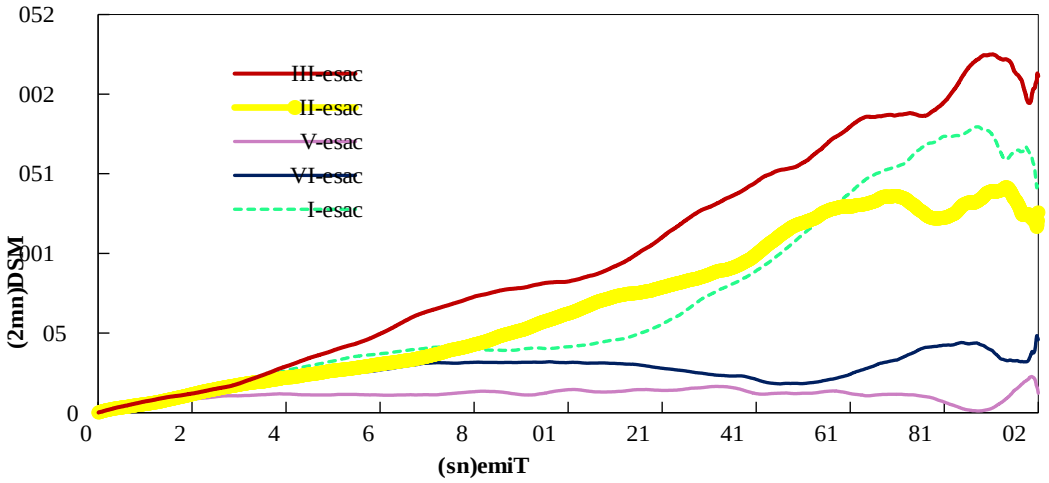


Figure (6) Mean square displacement (MSD) of the Aβ oligomer during the final 20 ns of each production trajectory.

Table 2. Apparent mobility coefficients of the Aβ oligomer obtained from MSD analysis over the final 20 ns of the production simulations.

system	MSD-derived apparent mobility coefficient (10^{-5} cm^2/s)
Case-I	2.1975
Case-II	1.8324
Case-III	2.9566
Case-IV	0.1320
Case-V	0.0269

The mobility values therefore reveal a clear compound-dependent effect of the electric field. The strongest response is obtained for bexarotene, supporting the hypothesis that the field modifies the molecular environment created by this compound and substantially alters the coupling between the peptide and membrane-associated environment. Because each condition was represented by a single trajectory, these values are interpreted here primarily as comparative, trajectory-based apparent mobility measures rather than as statistically converged ensemble diffusion coefficients. This distinction is important when interpreting the magnitude of the differences among the cases.

3.4. Spatial distribution of Aβ and the drug molecules

To determine whether the distinct mobility responses are related to differences in molecular localization, mass-density profiles were calculated for Aβ and the drug molecules. The results are shown in Figures 7 and 8. As shown in Fig. 7, the spatial distributions of Aβ and bexarotene exhibit greater overlap than those of Aβ and AC0107. This indicates a stronger spatial association between bexarotene and the peptide. In contrast, AC0107 displays a distribution that is more strongly associated with the membrane–peptide interfacial region. The density profile of the bexarotene-containing system in the presence of the electric field is also broader, indicating that the field modifies the spatial organization of the peptide–drug system.

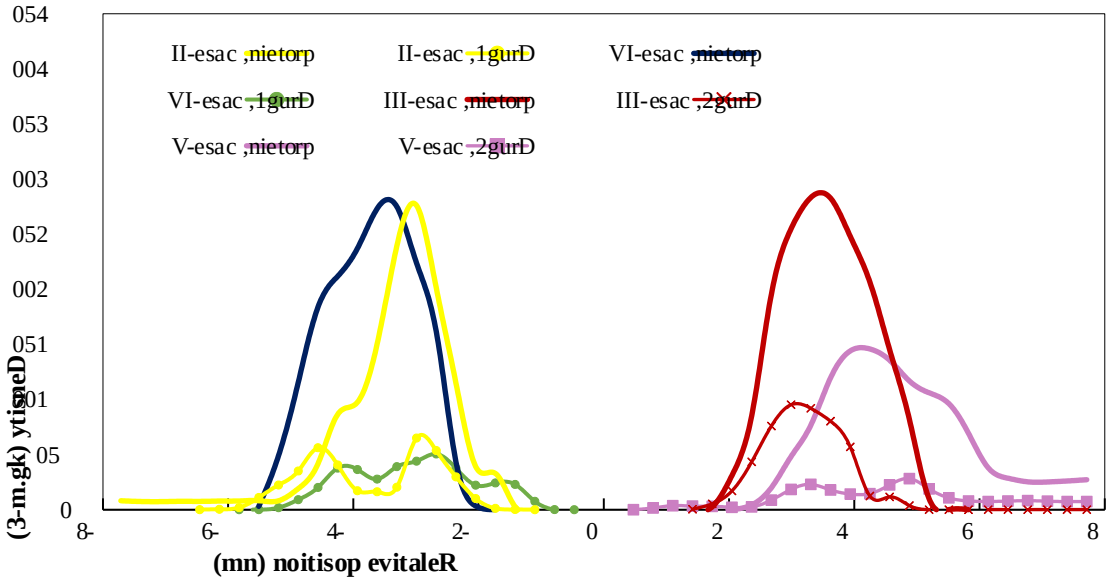


Figure (7) Mass-density profiles of the Aβ oligomer and drug molecules in the presence of AC0107 (left) and bexarotene (right) under the applied electric field (Cases IV and V).

The density profiles near the polar head-group region of the membrane, presented in Fig. 8, provide further information about peptide–membrane association. The overlap between the peptide and membrane density profiles is altered by both compounds, and the application of the electric field produces a particularly pronounced reduction in this overlap in the presence of bexarotene. This observation is consistent with weaker direct association between the peptide and membrane under Case V.

The combined density profiles therefore suggest two distinct spatial organizations. AC0107 preferentially occupies the region close to the membrane–peptide interface, whereas bexarotene preferentially remains associated with the peptide. These different localization patterns provide a plausible molecular explanation for the different mobility and membrane-interaction responses observed for the two compounds.

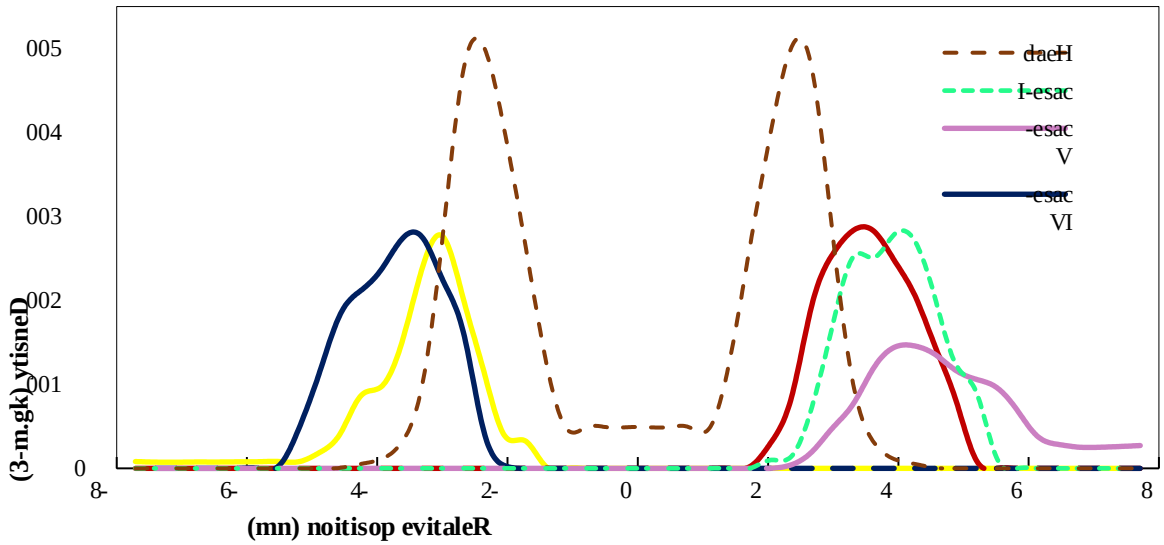


Figure (8) Mass-density profiles showing the spatial overlap between the Aβ oligomer and the polar head-group region of the membrane in the presence of AC0107 (left) and bexarotene (right), with and .without the applied electric field

3.5. Hydrogen-bonding interactions

Hydrogen bonding was analyzed over the final 20 ns of each production trajectory to quantify the interactions between Aβ, POPC, and the two compounds. The corresponding values are given in Tables 3–5.

The average numbers of hydrogen bonds between Aβ and POPC are 8.4, 13.650, 9.614, 12.374, and 5.847 for Cases I–V, respectively (Table 3). In the bexarotene-containing systems, the reported average number of Aβ–POPC hydrogen bonds decreases from 9.614 in Case III to 5.847 in Case V, a descriptive reduction of approximately 39%. In the AC0107-containing systems, the corresponding value decreases from 13.650 in Case II to 12.374 in Case IV, a descriptive reduction of approximately 9%. AC0107 therefore increases the number of Aβ–POPC hydrogen bonds in Case II, whereas bexarotene results in fewer peptide–membrane hydrogen bonds. The smallest value is obtained for Case V, where bexarotene is combined with the electric field. This result is consistent with the density-profile analysis and indicates a reduction in direct hydrogen-bond-mediated coupling between the Aβ oligomer and the lipid membrane.

The interaction of the compounds with POPC shows a complementary behavior (Table 4). AC0107 forms approximately 4.890 hydrogen bonds with POPC in Case II and 8.174 in Case IV, indicating stronger interaction with the membrane when the electric field is applied. In

contrast, the corresponding values for bexarotene decrease from 4.999 in Case III to 1.036 in Case V. These results suggest that the electric field promotes a stronger membrane association of AC0107 but markedly reduces direct bexarotene–POPC hydrogen bonding.

Table 3. The average number of hydrogen bonds between Aβ peptide and bilayer membrane in 5 systems in the last 20 nanoseconds of simulation.

system	No. of Hbond
protein & POPC(case-I)	**8.4**
protein & POPC(case-II)	**13.650**
protein & POPC(case-IV)	**12.374**
protein & POPC(case-III)	**9.614**
protein & POPC(case-V)	**5.847**

Table 4. Average number of hydrogen bonds between drug molecules and lipid bilayer membrane.

system	No. of Hbond
Drug1 & POPC(case-II)	**4.890**
Drug1 & POPC(case-IV)	**8.174**
Drug2 & POPC(case-III)	**4.999**
Drug2 & POPC(case-V)	**1.036**

Table 5. Average number of hydrogen bonds between drug molecules and amyloid beta peptide.

system	No. of Hbond
Drug1 & protein(caseII)	**4.629**
Drug1 & protein(caseIV)	**3.987**
Drug2 & protein(case-III)	**5.339**
Drug2 & protein(case-V)	**7.170**

The drug–Aβ interactions provide the complementary picture (Table 5). AC0107 forms 4.629 and 3.987 hydrogen bonds with Aβ in Cases II and IV, respectively. Bexarotene forms 5.339 hydrogen bonds in Case III and 7.170 in Case V. Thus, in the presence of the electric field, the interaction between bexarotene and Aβ becomes particularly pronounced, while the direct interaction between bexarotene and the membrane is strongly reduced.

The hydrogen-bonding data therefore support a clear mechanistic distinction between the two compounds. AC0107 preferentially maintains a strong interaction with the membrane–peptide interface, whereas bexarotene shows a stronger preference for association with Aβ, particularly under the applied electric field.

3.6. Radial distribution functions and molecular localization

To further characterize the relative positions of the peptide, the compounds, and the membrane, RDFs were calculated for selected atom pairs. The results are presented in Figure 9.

The peptide–drug RDF in Fig. 9a indicates that bexarotene has a higher probability of being located close to Aβ than AC0107. In contrast, the drug–membrane RDF shown in Fig. 9b indicates a stronger localization of AC0107 near membrane phosphorus atoms. The RDF between peptide and membrane atoms in Figure 9c further suggests that AC0107 alters the spatial relationship between the peptide and membrane. When combined with the mass-density and hydrogen-bonding results, these observations support two different modes of molecular localization. AC0107 preferentially accumulates near the membrane–peptide interface and maintains substantial interaction with the lipid bilayer. This arrangement is consistent with a barrier-like interfacial mechanism, in which the molecule modifies direct peptide access to the membrane surface.

Bexarotene exhibits a different spatial preference. Its stronger association with Aβ, combined with the reduced Aβ–POPC hydrogen bonding and reduced peptide–membrane density overlap observed in Case V, is consistent with preferential peptide association and weaker direct peptide–membrane coupling.

We therefore interpret the two compounds as producing distinct interaction environments rather than as acting through a single common mechanism. The RDF analysis is especially useful in establishing this distinction because it directly connects the molecular-scale spatial distribution to the changes observed in peptide mobility and hydrogen bonding.

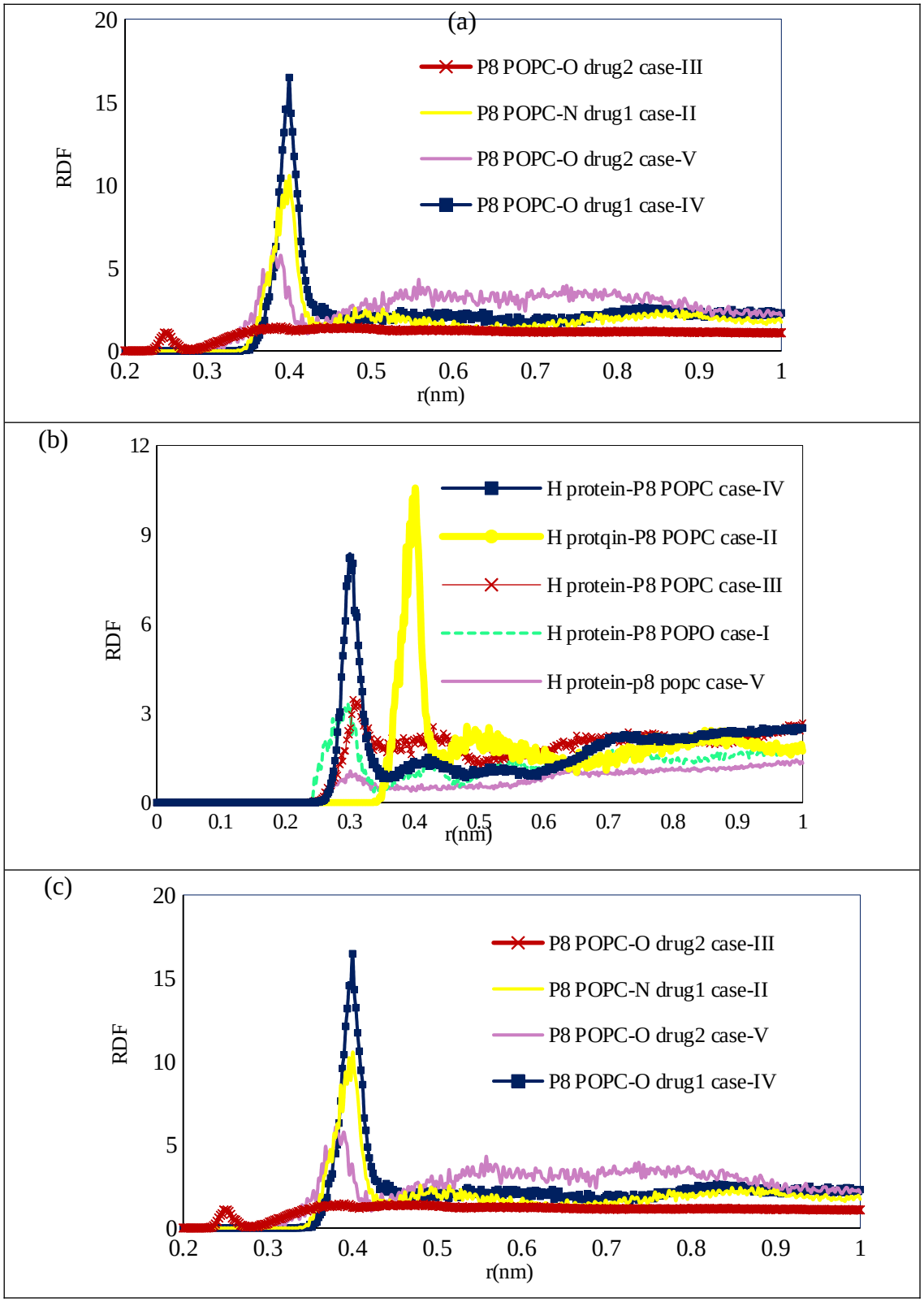


Figure (9) Radial distribution functions (RDFs) describing drug–peptide, drug–membrane, and peptide–membrane spatial organization.

3.7. Integrated mechanistic interpretation

The combined results from Figures 3–9 provide a consistent molecular picture of the response of membrane-associated Aβ to AC0107, bexarotene, and the applied GHz electric field.

AC0107 primarily modifies the membrane–peptide interfacial environment. It increases local Aβ fluctuations, enhances interactions with POPC, and preferentially occupies the region between the peptide and membrane. These observations are consistent with an interfacial, barrier-like mechanism rather than a simple destabilization of the peptide structure.

Bexarotene exhibits a different behavior. It preferentially associates with Aβ, reduces direct peptide–membrane hydrogen bonding, and becomes particularly strongly associated with the peptide in the presence of the electric field. The corresponding Case V also exhibits the lowest MSD-derived mobility and the reduced peptide–membrane density overlap. The agreement among these independent observables strengthens the interpretation that bexarotene substantially modifies the membrane association of the Aβ oligomer under the applied field.

An important result is therefore that the electric field does not produce an identical response for the two compounds. Instead, it differentially modulates the molecular interaction networks established by AC0107 and bexarotene. The strongest field-dependent response is observed for bexarotene, for which increased peptide association is accompanied by reduced direct peptide–membrane interaction and markedly restricted apparent mobility.

Overall, the results suggest that molecular localization is a key determinant of how an external electric-field perturbation influences membrane-associated Aβ. The distinct responses of AC0107 and bexarotene highlight the importance of considering drug–membrane–peptide interactions collectively rather than evaluating peptide aggregation or drug binding as isolated processes.

4. Conclusion

In this study, atomistic molecular dynamics simulations were used to investigate how AC0107 and bexarotene modulate the interactions of Aβ oligomers with a cholesterol-enriched POPC membrane, and how these effects are altered by an oscillating GHz electric field. Five computational conditions were examined, and complementary structural, dynamical, and

intermolecular analyses were used to characterize the response of the peptide–membrane systems.

The simulations reveal distinct molecular behaviors for the two compounds. AC0107 preferentially localizes at the peptide–membrane interface and exhibits enhanced interaction with the lipid bilayer, including an increase in Aβ–POPC and AC0107–POPC hydrogen bonding. Its spatial distribution is therefore consistent with a barrier-like interfacial mechanism that modifies the direct association of the peptide with the membrane. In contrast, Bexarotene preferentially associates with the Aβ oligomer, and when the electric field is applied, it reduces Aβ–membrane hydrogen bonding, which is together with a substantial reduction in the apparent peptide mobility. The electric field therefore produces a compound-dependent response rather than a uniform effect on the Aβ–membrane system. In particular, the combination of bexarotene and the applied field results in the strongest reduction in peptide mobility and the weakest direct peptide–membrane interaction among the investigated conditions. These observations, together with the density and RDF analyses, support a mechanistic picture in which molecular localization plays a central role in determining the response of Aβ–membrane assemblies to an external electric-field perturbation.

Overall, the present results provide molecular-level insight into the interplay among Aβ oligomers, lipid membranes, small molecules, and external electric fields. The findings may serve as a computational basis for future studies aimed at experimentally testing compound-dependent modulation of membrane-associated Aβ behavior.

5. Limitations

A limitation of the present work is that each simulation condition was represented by a single molecular dynamics trajectory. This was primarily due to the substantial computational cost of the combined Aβ–membrane–drug systems under an oscillating electric field. Consequently, the reported quantities should be interpreted primarily in terms of comparative trends and mechanistic consistency within the simulated trajectories, rather than as fully converged ensemble averages with rigorously estimated uncertainties.

To partially address this limitation, relatively long simulations were performed for each condition, consisting of 200 ns equilibration followed by 200 ns production, and the

interpretation was based on several complementary observables, including RMSD, RMSF, Rg, MSD, membrane ordering, density profiles, hydrogen bonding, and RDFs.

The conclusions should therefore be considered as mechanistic insights generated under the specified model conditions. Future studies involving multiple independent replicas, alternative membrane compositions, and broader sampling would be valuable for quantifying statistical uncertainties and testing the generality of the observed trends.

Author contributions

Nafiseh Salehi: Investigation, Methodology, Writing-Original Draft, Visualization, Software, Formal analysis, Data curation.

Amir Lohrasebi: Conceptualization, Investigation, Methodology, Validation, Draft preparation, Resources, Writing-reviewing, and Editing.

Statements and Declarations:

Funding Declaration

No funding was received to assist with the preparation of this manuscript.

Conflicts of interest

There are no conflicts to declare.

Data availability

The data supporting the findings of this study are available upon request from the corresponding author.

AI disclosure statement

During the preparation of this manuscript, the authors used ChatGPT-6, OpenAI to improve the readability and language of the manuscript. After using this tool, the authors reviewed and edited the content as needed and take full responsibility for the content of the publication.

Acknowledgments

Declared none.

References

[1] Hardy, J. A.; Higgins, G. A. Alzheimer's disease: The amyloid cascade hypothesis. Science 1992, 256 (5054), 184–185. https://doi.org/10.1126/science.1566067.

[2] Tachi, Y.; Itoh, S. G.; Okumura, H. Molecular dynamics simulations of amyloid-β peptides in heterogeneous environments. Biophys. Physicobiol. 2022, 19, e190010. https://doi.org/10.2142/biophysico.bppb-v19.0010.

[3] Nguyen, P. H.; Sterpone, F.; Derreumaux, P. Self-assembly of amyloid-β (Aβ) peptides from solution to near in vivo conditions. J. Phys. Chem. B 2022, 126 (49), 10317–10326. https://doi.org/10.1021/acs.jpcb.2c06375.

[4] Salehi, N.; Lohrasebi, A.; Rezaeisaadaat, M.; Bordbar, A. K. The influences of cholesterol and AC0107 inhibitor molecules on the amyloid-beta fibrils aggregation in cell membranes: Molecular modeling approach. Eur. Phys. J. Plus 2022, 137 (4), 460. https://doi.org/10.1140/epjp/s13360-022-02681-z.

[5] Zou, Y.; Qian, Z.; Chen, Y.; Qian, H.; Wei, G.; Zhang, Q. Norepinephrine inhibits Alzheimer's amyloid-β peptide aggregation and destabilizes amyloid-β protofibrils: A molecular dynamics simulation study. ACS Chem. Neurosci. 2019, 10 (3), 1585–1594. https://doi.org/10.1021/acschemneuro.8b00537.

[6] Atanasova, M. Small-molecule inhibitors of amyloid beta: Insights from molecular dynamics—Part A: Endogenous compounds and repurposed drugs. Pharmaceuticals 2025, 18 (3), 306. https://doi.org/10.3390/ph18030306.

[7] Downey, M. A.; Giammona, M. J.; Lang, C. A.; Buratto, S. K.; Singh, A.; Bowers, M. T. Inhibiting and remodeling toxic amyloid-beta oligomer formation using a computationally designed drug molecule that targets Alzheimer's disease. J. Am. Soc. Mass Spectrom. 2019, 30 (1), 85–93. https://doi.org/10.1007/s13361-018-1975-1.

[8] Sofińska, K.; Batys, P.; Cernescu, A.; Ghosh, D.; Skirlińska-Nosek, K.; Barbasz, J.; Seweryn, S.; Wilkosz, N.; Riek, R.; Szymoński, M.; Lipiec, E. Nanoscale insights into the local structural rearrangements of amyloid-β induced by bexarotene. Nanoscale 2023, 15 (35), 14606–14614. https://doi.org/10.1039/D3NR01608K.

[9] Cramer, P. E.; Cirrito, J. R.; Wesson, D. W.; Lee, C. Y. D.; Karlo, J. C.; Zinn, A. E.; Casali, B. T.; Restivo, J. L.; Goebel, W. D.; James, M. J.; Brunden, K. R.; Wilson, D. A.; Landreth, G. E. ApoE-directed therapeutics rapidly clear β-amyloid and reverse deficits in AD mouse models. Science 2012, 335 (6075), 1503–1506. https://doi.org/10.1126/science.1217697.

[10] Fantini, J.; Di Scala, C.; Yahi, N.; Troadec, J. D.; Sadelli, K.; Chahinian, H.; Garmy, N. Bexarotene blocks calcium-permeable ion channels formed by neurotoxic Alzheimer's β-amyloid peptides. ACS Chem. Neurosci. 2014, 5 (3), 216–224. https://doi.org/10.1021/cn400183w.

[11] Salehi, N.; Lohrasebi, A.; Bordbar, A. K. Preventing the amyloid-beta peptides accumulation on the cell membrane by applying GHz electric fields: A molecular dynamic simulation. J. Mol. Graph. Model. 2023, 123, 108516. https://doi.org/10.1016/j.jmgm.2023.108516.

[12] Vargas-Rosales, P. A.; D'Addio, A.; Zhang, Y.; Caflisch, A. Disrupting dimeric β-amyloid by electric fields. ACS Phys. Chem. Au 2023, 3 (5), 456–466. https://doi.org/10.1021/acsphyschemau.3c00021.

[13] Salimi, A.; Chatterjee, S.; Lee, J. Y. Exposure to the electric field: A potential way to block the aggregation of histidine tautomeric isomers of β-amyloid. Int. J. Biol. Macromol. 2023, 232, 123385. https://doi.org/10.1016/j.ijbiomac.2023.123385.

[14] Wu, R.; Ou, X.; Zhang, L.; Song, X.; Wang, Z.; Dong, M.; Liu, L. Electric field effect on inhibiting the co-fibrillation of amyloid peptides by modulating the aggregation pathway. Langmuir 2022, 38 (40), 12346–12355. https://doi.org/10.1021/acs.langmuir.2c02055.

[15] Saikia, J.; Pandey, G.; Sasidharan, S.; Antony, F.; Nemade, H. B.; Kumar, S.; Chaudhary, N.; Ramakrishnan, V. Electric field disruption of amyloid aggregation: Potential noninvasive therapy for Alzheimer's disease. ACS Chem. Neurosci. 2019, 10 (5), 2250–2262. https://doi.org/10.1021/acschemneuro.8b00490.

[16] Todorova, N.; Bentvelzen, A.; Yarovsky, I. Electromagnetic field modulates aggregation propensity of amyloid peptides. J. Chem. Phys. 2020, 152 (3), 035104. https://doi.org/10.1063/1.5126367.

[17] Topology Builder (ATB) and repository: version 1.0. Journal of Chemical Theory and Computation. 2011;7(12):4026–4037. https://doi.org/10.1021/ct200196m.

[18] Chitranshi, N.; Dheer, Y.; Kumar, S.; Graham, S. L.; Gupta, V. Molecular docking, dynamics, and pharmacology studies on bexarotene as an agonist of ligand-activated transcription factors, retinoid X receptors. J. Cell. Biochem. 2019, 120 (7), 11745–11760. https://doi.org/10.1002/jcb.28455.

[19] Huang, W.; Lin, Z.; van Gunsteren, W. F. Validation of the GROMOS 54A7 force field with respect to β-peptide folding. J. Chem. Theory Comput. 2011, 7 (5), 1237–1243. https://doi.org/10.1021/ct100747y.

[20] Mark, P.; Nilsson, L. Structure and dynamics of the TIP3P, SPC, and SPC/E water models at 298 K. J. Phys. Chem. A 2001, 105 (43), 9954–9960. https://doi.org/10.1021/jp003020w.

[21] Essmann, U.; Perera, L.; Berkowitz, M. L.; Darden, T.; Lee, H.; Pedersen, L. G. A smooth particle mesh Ewald method. J. Chem. Phys. 1995, 103 (19), 8577–8593. https://doi.org/10.1063/1.470117.

[22] Evans, D. J.; Holian, B. L. The Nosé–Hoover thermostat. J. Chem. Phys. 1985, 83 (8), 4069–4074. https://doi.org/10.1063/1.449071.

[23] Parrinello, M.; Rahman, A. Polymorphic transitions in single crystals: A new molecular dynamics method. J. Appl. Phys. 1981, 52 (12), 7182–7190. https://doi.org/10.1063/1.328693.